

A New Series of Proton/Charge Transfer Molecules: Synthesis and Spectral Studies of 2-(5-Aryl-1-carbomethoxy-1H-pyrazol-3-yl)phenols

Mary E. Rampey, Carrie E. Halkyard, Angela R. Williams, April J. Angel, Douglas R. Hurst, Jessica D. Townsend, Anne E. Finefrock, Charles F. Beam* and Shannon L. Studer-Martinez*

Department of Chemistry and Biochemistry, College of Charleston, Charleston, SC, USA

Received 4 February 1999; accepted 18 May 1999

ABSTRACT

The carbomethoxyhydrazone of 2'-hydroxyacetophenone was trilitiated with excess lithium diisopropylamide and C-acylated with a variety of benzoate esters followed by acid cyclization of the intermediates to 2-(5-aryl-1-carbomethoxy-1H-pyrazol-3-yl)phenols [3-(2-hydroxyphenyl)-1H-pyrazoles]. The products were characterized by Fourier transform-IR, ¹H NMR, ¹³C NMR, UV-visible absorption and fluorescence. All the derivatives in *n*-heptane have an absorption maximum at ~304 nm and an extremely weak ($\Phi_f = 10^{-4}$) fluorescence with maxima in the range of 335–460 nm. The broad range of fluorescence maxima and fluorescence quantum yields is attributed to varying contributions of charge transfer that are dependent on both the identity of the substituent and solvent polarity. A phenomenally large Stokes-shifted fluorescence maximum at 620 nm was observed for 2-(1-carbomethoxy-5-[4-dimethylaminophenyl]-1H-pyrazol-3-yl)phenol in *n*-heptane and attributed to excited-state intramolecular proton transfer. As a result, competitive excited-state proton/charge transfer properties have been observed in the pyrazoles studied, of which the spectral properties can be fine tuned by substituent as well as solvent effects.

INTRODUCTION

There has been a great deal of current interest in both excited-state intramolecular proton transfer (ESIPT)[†] (1–6) and charge transfer (ESICT) (7–11) in order to shed light on their photophysical dynamics and their affect on one another (12–17). The ESIPT involves the intramolecular transfer of a hydroxyl or amino proton to an accepting site on the molecule such as carbonyl oxygen or another nitrogen while the molecule is in the excited state. The resulting structure

change manifests itself in a large Stokes shift between the absorption and emission maxima. Alternatively, ESIPT involves the redistribution of electron density between a donor and acceptor site on the molecule in the excited state. In response, a charge transfer state of lower energy is formed through solvent dielectric relaxation, which relaxes to its Franck–Condon ground state, resulting in a large Stokes-shifted emission. Due to negligible reabsorption, these molecules are potential candidates for use in practical applications such as laser dyes (12,18–21), special Raman filters (22), switches for dye laser pulse shortening (23) and hard-scintillator counters (24). Another interesting application is using ESIPT or ESIPT molecules as fluorescence probes to investigate a variety of biological environments such as a protein's binding site (25–30). Recently, Catalan *et al.* have also looked at *N*-(2'-hydroxyphenyl)pyrazoles that undergo ESIPT and their ability to photoprotect polystyrene (5,6).

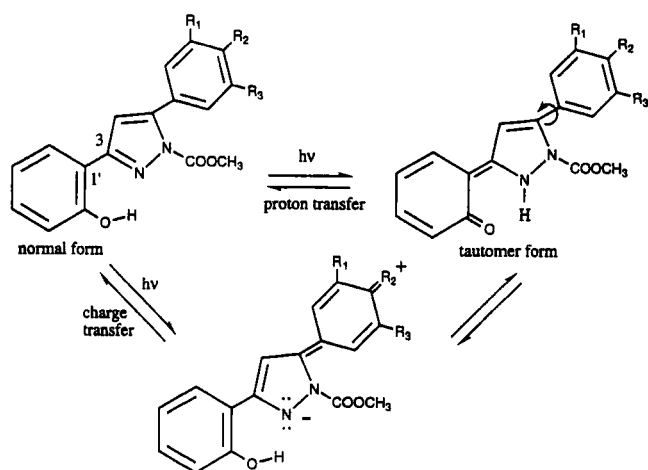
While investigating the dependence of ESIPT and ESIPT on one another, several groups have found that placing an electron-donating group in the 4'-position of the 2-phenyl ring of 3-hydroxyflavone significantly influences the photophysical properties of this molecule (15–17). Chou *et al.* proposed that solvent dielectric perturbation could reverse the relative energies of proton transfer *versus* charge transfer, making proton transfer energetically unfavorable (15). Ormson *et al.* observed a substantial increase in the fluorescence quantum yield of 4'-*N,N*-dimethylamino-3-hydroxyflavone in polar solvents and proposed that twisted intramolecular charge transfer was competing with proton transfer (17). These studies show that substituents in resonance positions definitely have the ability to influence absorption and emission maxima and, in turn, the dominant processes occurring in the excited state.

Our investigation has involved the synthesis and spectroscopic characterization of a series of new 3-(2-hydroxyphenyl)-1H-pyrazoles. The basic structure of these compounds is similar, especially in the placement of the 2-hydroxyphenyl pendant group, to those studied by Catalan *et al.* Catalan's investigation focused on the effects of intramolecular hydrogen bonding (IMHB) and torsional motion about a central carbon–carbon bond as opposed to a carbon–nitrogen bond on the photostability of 3- and 5-(2'-hydroxyphenyl)pyrazoles. The compounds reported in this study are different from those used by Catalan *et al.* due to the introduction of substituents that create the potential for ESIPT

*To whom correspondence should be addressed at: Department of Chemistry and Biochemistry, College of Charleston, Charleston, SC 29424, USA. Fax: 843-953-1404; e-mail: beamc@cofc.edu or mmartnz@sprynet.com

[†]Abbreviations: DMSO, dimethylsulfoxide; ESIPT, excited-state intramolecular charge transfer; ESIPT, excited-state intramolecular proton transfer; FT, Fourier transform; IMHB, intramolecular hydrogen bonding; LDA, lithium diisopropylamide; m.p., melting point; THF, tetrahydrofuran; TMS, tetramethylsilane.

© 1999 American Society for Photobiology 0031-8655/99 \$5.00+0.00



Scheme 1. The normal form of 3-(2-hydroxyphenyl)-1H-pyrazoles and the tautomer form resulting from ESIPT. Also shown is the resonance-contributing structure that is produced following charge transfer.

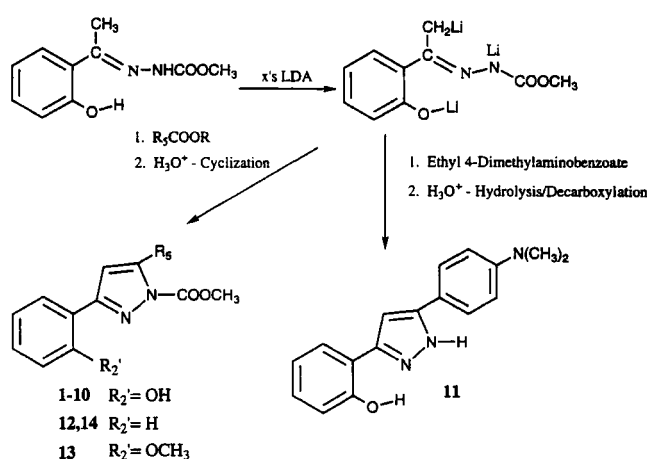
along with ESIPT. Scheme 1 shows the general structure of the compounds studied and the tautomer that would result from proton transfer. The series of molecules (1–11) provide an opportunity to examine the correlation between electron-donating and withdrawing groups placed in resonance and nonresonance positions on the 5-phenyl substituent of the pyrazole ring and the resulting physical characteristics. Scheme 1 also shows a charge transfer intermediate that could play a role in ESIPT for the case that R_2 is an electron-donating group. The partial negative charge on the pyrazole nitrogen (N-2) will make it a more attractive proton acceptor, while the increased double bond character between the pyrazole and the phenyl ring will minimize nonradiative decay through torsional motion (14). Both these factors support our results that ESIC can be a driving force for ESIPT. Another observation based on the spectroscopic properties of derivatives 12–14, is that IMHB is a significant nonradiative pathway that facilitates relaxation from the $S_1 \rightarrow S_0$ states of the normal form.

MATERIALS AND METHODS

Synthesis

Melting points (m.p.) were obtained with a Mel-Temp II melting point apparatus in open capillary tubes and are uncorrected. Fourier transform (FT) IR spectra were obtained on a Nicolet Impact 410 FT-IR. Proton and C-13 NMR spectra were obtained with a Varian Associates Mercury Oxford 300 MHz NMR spectrometer, and chemical shifts are recorded in δ ppm downfield from an internal tetramethylsilane (TMS) standard. Combustion analyses for C, H and N were performed by Quantitative Technologies, Inc., P.O. Box 470, Salem Industrial Park, Bldg. 5, Whitehouse, NJ 08888. The tetrahydrofuran (THF) was distilled from sodium (benzophenone ketyl) prior to use, and additional chemicals were obtained from Aldrich Chemical Co.

Preparation of entry compound: (1-[2-hydroxyphenyl]-ethylidene)hydrazinecarboxylic acid, methyl ester. The carbomethoxyhydrazone was prepared by a well-documented procedure (31), where methyl hydrazinecarboxylate (0.10 mol) and 2'-hydroxyacetophenone (0.10 mol) were heated with stirring under reflux (1–1.5 h) in methanol (100 mL) containing a small amount of acetic acid (1 mL). Upon reduction of the volume to 40–50 mL and cooling, crystallization usually occurred, but it could be aided by addition of a few ice crystals. After filtration and drying, 10.6 g (51% yield) of product



Scheme 2. Preparation of 3-(2-hydroxyphenyl)-1H-pyrazoles 1–11 and 3-(2-phenyl)-1H-pyrazoles 12, 14 and 3-(2-methoxyphenyl)-1H-pyrazole 13.

was obtained, and it was usually pure enough for the lithiation procedures. The work-up of a second crop of the crystalline product was not pursued. It could be recrystallized from methanol; m.p. = 172–175°C FT-IR (paraffin oil) 3290, 1730 and 1711 cm^{-1} . $^1\text{H-NMR}$ (dimethylsulfoxide [DMSO-d_6]): δ 2.317 (3H, s), 3.772 (3H, s), 6.866–7.558 (4H, m) and 10.792 (1H, s). $^{13}\text{C-NMR}$ (DMSO-d_6): δ 13.2, 52.1, 116.7, 118.1, 119.1, 127.6, 130.2, 154.1 and 157.7. Analysis calculated for $\text{C}_{10}\text{H}_{12}\text{N}_2\text{O}_3$: C, 57.69; H, 5.81; N, 13.45. Found: C, 57.72; H, 5.75; N, 13.45.

General experimental procedure for preparing 2-(5-aryl-1-carbomethoxy-1H-pyrazol-3-yl)phenols 1–14. In a typical experiment, 2'-hydroxyacetophenone carbomethoxyhydrazone [1-(2-hydroxyphenyl)ethylidene]hydrazinecarboxylic acid, methyl ester) for 1–11 (acetophenone carbomethoxyhydrazone for 12 and 14 and 2'-methoxyacetophenone carbomethoxyhydrazone for 13) was added to excess lithium diisopropylamide (LDA), followed by a salicylate ester (hydrazone: base: ester, 1:5:1 for 1–8, 1:6:1 for 9–11, 1:3:1 for 12 and 13 and 1:4:1 for 14) (~5% excess was used for making LDA and the ester used) and then acid-cyclization to the product (Scheme 2).

The LDA was prepared by adding 5.37 g (0.0525 mol for 1–8) or 6.43 g (0.0630 mol for 9–11) or 3.22 g (0.0315 mol for 12 and 13) or 4.29 g (0.0420 mol for 14) of diisopropylamine, dissolved in 45–55 mL of dry THF to 33 mL (0.0525 mol for 1–8) or 39 mL (0.0630 mol for 9–11) or 20 mL (0.0315 mol for 12 and 13) or 27 mL (0.0420 mol for 14) of 1.6 M *n*-butyllithium (N_2 , 0°C). After 20 min, 2.08 g (0.0100 mol) of the 2'-hydroxyacetophenone carbomethoxyhydrazone for 1–11, acetophenone carbomethoxyhydrazone for 12 and 14, or 2-methoxyacetophenone carbomethoxyhydrazone for 13, dissolved in 35–45 mL of dry THF, was added at a fast dropwise rate (5 min). After stirring at 0°C for 2 h, 0.0105 mol of benzoate ester, dissolved in 25–35 mL of dry THF, was added at a fast dropwise rate (5 min), and the resulting mixture was stirred at 0°C for an additional 1 h (1.5 h for 9–11 and 14). The mixture was quenched by addition of 100 mL of 3 N hydrochloric acid, and the resulting two-phase mixture was stirred and heated under reflux for 1 h. The mixture was then poured into a large flask (1 L) containing ice (~100 g), and after adding solvent-grade ether (~100 mL), it was neutralized with solid sodium bicarbonate. The layers were separated, the aqueous layer was extracted with ether or THF (2 \times 75 mL) and the ether extracts were combined and evaporated.

2-(1-Carbomethoxy-5-phenyl-1H-pyrazole-3-yl)phenol (1). This compound was prepared by the general procedure described from 0.0100 mol of hydrazone; 1.38 g, 47% yield, m.p. = 161–162°C (methanol/water). FT-IR (paraffin oil): 1728 cm^{-1} . $^1\text{H-NMR}$ (CDCl_3): δ 3.949 (3H, s), 6.780 (1H, s), 6.917–7.583 (9H, m) and 10.704 (1H, s). $^{13}\text{C-NMR}$ (CDCl_3): δ 55.0, 108.7, 115.0, 117.7, 119.6, 127.4, 128.2, 129.0, 129.3, 130.1, 140.0, 147.9, 150.0, 154.2 and 157.0. Analysis calculated for $\text{C}_{17}\text{H}_{14}\text{N}_2\text{O}_3$: C, 69.38; H, 4.79; N, 9.52. Found: C, 69.09; H, 5.06; N, 9.62.

2-(1-Carbomethoxy-5-[4-methylphenyl]-1H-pyrazol-3-yl)phenol (2). This compound was prepared by the general procedure described from 0.0100 mol of hydrazone; 2.71 g, 88% yield, m.p. = 167–169°C (methanol/toluene). FT-IR (paraffin oil): 1759 cm⁻¹. ¹H-NMR (CDCl₃): δ 2.419 (3H, s), 3.954 (3H, s), 6.751 (1H, s), 6.909–7.579 (8H, m) and 10.732 (1H, s). ¹³C-NMR (CDCl₃): δ 21.8, 55.0, 108.4, 115.1, 117.7, 119.6, 127.2, 127.4, 128.6, 129.2, 130.9, 139.6, 148.1, 150.0, 154.2, and 157.0. Analysis Calculated for C₁₈H₁₆N₂O₃: C, 70.12; H, 5.23; N, 9.09. Found: C, 70.42; H, 5.41; N, 8.78.

2-(5-[4-Chlorophenyl]-1-carbomethoxy-1H-pyrazol-3-yl)phenol (3). This compound was prepared by the general procedure described from 0.0100 mol of hydrazone; 2.10 g, 64% yield, m.p. = 133–135°C (methanol/water). FT-IR (paraffin oil): 1757 cm⁻¹. ¹H-NMR (CDCl₃): δ 3.965 (3H, s), 6.776 (1H, s), 6.915–7.572 (8H, m) and 10.626 (1H, s). ¹³C-NMR (CDCl₃): δ 55.1, 108.8, 114.8, 117.7, 119.6, 127.4, 128.5, 130.6, 131.1, 135.7, 146.7, 149.9, 154.3 and 156.9. Analysis calculated for C₁₇H₁₃ClN₂O₃: C, 62.11; H, 3.99; N, 8.52. Found: C, 61.91; H, 4.14; N, 8.48.

2-(5-[4-Bromophenyl]-1-carbomethoxy-1H-pyrazol-3-yl)phenol (4). This compound was prepared by the general procedure described from 0.0100 mol of hydrazone; 2.91 g, 78% yield, m.p. = 140–142°C (ethanol/benzene). FT-IR (paraffin oil): 1727 cm⁻¹. ¹H-NMR (CDCl₃): δ 3.968 (3H, s), 6.780 (1H, s), 6.918–7.613 (8H, m), and 10.623 (1H, s). ¹³C-NMR (CDCl₃): δ 55.0, 108.77, 114.7, 117.6, 119.5, 123.9, 127.3, 128.9, 130.8, 131.0, 131.3, 146.6, 149.7, 154.2 and 156.8. Analysis calculated for C₁₇H₁₃BrN₂O₃: C, 54.71; H, 3.51; N, 7.51. Found: C, 54.79; H, 3.52; N, 7.49.

2-(1-Carbomethoxy-5-[3,5-dimethoxyphenyl]-1H-pyrazol-3-yl)phenol (5). This compound was prepared by the general procedure described from 0.0100 mol of hydrazone; 2.34 g, 66% yield, m.p. = 149–150°C (methanol/water). FT-IR (paraffin oil): 1753 cm⁻¹. ¹H-NMR (CDCl₃): δ 3.822 (6H, s), 3.968 (3H, s), 6.549–6.603 (3H, m), 7.783 (1H, s), 6.915–7.579 (4H, m) and 10.684 (1H, s). ¹³C-NMR (CDCl₃): δ 55.1, 55.7, 101.4, 107.6, 108.6, 115.0, 117.7, 119.6, 127.4, 131.0, 131.8, 147.7, 149.7, 154.1, 156.9 and 160.4. Analysis calculated for C₁₉H₁₈N₂O₅: C, 64.40; H, 5.12; N, 7.91. Found: C, 64.26; H, 5.12; N, 7.75.

2-(1-Carbomethoxy-5-[4-methoxyphenyl]-1H-pyrazol-3-yl)phenol (6). This compound was prepared by the general procedure described from 0.0100 mol of hydrazone; 3.05 g, 94% yield, m.p. = 156–158°C (methanol/toluene). FT-IR (paraffin oil): 1726 cm⁻¹. ¹H-NMR (CDCl₃): δ 3.855 (3H, s), 3.956 (3H, s), 6.732 (1H, s), 6.931–7.577 (8H, m) and 10.742 (1H, s). ¹³C-NMR (CDCl₃): δ 54.9, 55.5, 108.2, 113.5, 115.0, 117.5, 119.4, 122.1, 127.3, 130.6, 130.8, 147.9, 149.9, 154.1, 156.9 and 160.4. Analysis calculated for C₁₈H₁₆N₂O₄: C, 66.66; H, 4.97; N, 8.64. Found: C, 66.41; H, 4.97; N, 8.58.

2-(1-Carbomethoxy-5-[3,4-dimethoxyphenyl]-1H-pyrazol-3-yl)phenol (7). This compound was prepared by the general procedure described from 0.0100 mol of hydrazone; 1.38 g, 39% yield, m.p. = 169–170°C (methanol/water). FT-IR (paraffin oil): 1763 cm⁻¹. ¹H-NMR (CDCl₃): δ 3.915 (3H, s), 3.940 (3H, s), 3.971 (3H, s), 6.765 (1H, s), 6.916–7.591 (7H, m) and 10.736 (1H, s). ¹³C-NMR (CDCl₃): δ 55.0, 56.2, 56.3, 108.4, 110.6, 112.6, 115.0, 117.6, 119.6, 122.2, 122.4, 127.4, 131.0, 147.9, 148.4, 149.905, 149.973, 154.1 and 157.0. Analysis calculated for C₁₉H₁₈N₂O₅: C, 64.40; H, 5.12; N, 7.91. Found: C, 64.31; H, 5.19; N, 7.94.

2-(1-Carbomethoxy-5-[3,4,5-trimethoxyphenyl]-1H-pyrazol-3-yl)phenol (8). This compound was prepared by the general procedure described from 0.0100 mol of hydrazone; 2.96 g, 77% yield, m.p. = 178–179°C (methanol/water). FT-IR (paraffin oil): 1762 cm⁻¹. ¹H-NMR (CDCl₃): δ 3.891 (6H, s), 3.922 (3H, s), 3.986 (3H, s), 6.696 (2H, s), 6.788 (1H, s), 6.925–7.591 (4H, m) and 10.690 (1H, s). ¹³C-NMR (CDCl₃): δ 55.1, 56.5, 61.2, 106.9, 108.7, 114.9, 117.8, 119.6, 125.3, 127.4, 131.0, 139.0, 147.8, 149.8, 152.9, 154.1 and 157.0. Analysis calculated for C₂₀H₂₀N₂O₆: C, 62.49; H, 5.24; N, 7.29. Found: C, 62.63; H, 5.26; N, 7.30.

2-(5-[4-Aminophenyl]-1-carbomethoxy-1H-pyrazol-3-yl)phenol (9). This compound was prepared by the general procedure described from 0.0100 mol of hydrazone; 1.21 g, 39% yield, m.p. = 193–195°C (methanol/toluene). FT-IR (paraffin oil): 3476, 3373 and 1756 cm⁻¹. ¹H-NMR (DMSO-d₆): δ 3.902 (3H, s), 5.476 (s), 6.600–6.658, 6.942–7.888 (9H, m) and 10.549 (1H, s). ¹³C-NMR (DMSO-d₆): δ 54.6, 108.5, 112.7, 116.0, 116.4, 116.6, 119.3, 127.9, 129.9, 130.3, 148.2, 149.5, 149.6, 152.3 and 155.8. Analysis calculated for

C₁₇H₁₅N₃O₃: C, 66.01; H, 4.89; N, 13.58. Found: C, 65.74; H, 4.97; N, 13.26.

2-(1-Carbomethoxy-5-[4-dimethylaminophenyl]-1H-pyrazol-3-yl)phenol (10). This compound was prepared by the general procedure described from 0.0100 mol of hydrazone; 2.22 g, 66% yield, m.p. = 160–162°C (95% ethanol). FT-IR (paraffin oil): 1763 cm⁻¹. ¹H-NMR (CDCl₃): δ 3.012 (6H, s), 3.966 (3H, s), 6.697 (1H, s), 6.727–7.582 (8H, m) and 10.838 (1H, s). ¹³C-NMR (CDCl₃): δ 40.4, 54.8, 107.4, 111.2, 115.2, 116.8, 117.5, 119.4, 127.3, 130.2, 130.7, 148.9, 150.1, 150.9, 154.1 and 156.9. Analysis calculated for C₁₉H₁₉N₃O₃: C, 67.64; H, 5.68; N, 12.45. Found: C, 67.74; H, 5.74; N, 12.40.

2-(5-[4-Dimethylaminophenyl]-1H-pyrazol-3-yl)phenol (11). This compound was prepared by the general procedure described from 0.0100 mol of hydrazone. After addition of 100 mL of 3 N hydrochloric acid and stirring and heating under reflux for 1 h, the mixture was cooled to room temperature and stirred for an additional 96 h. The work-up was the same as described in the general procedure; 2.21 g, 79% yield, m.p. = 211–212°C (benzene/95% ethanol). FT-IR (paraffin oil): 3404, 1616 and 1587 cm⁻¹. ¹H-NMR (DMSO-d₆): δ 2.979 (6H, s), 6.817–7.398, 7.690–7.812 (9H, m), 11.186 (1H, s) and 13.431 (1H, s). ¹³C-NMR (DMSO-d₆): δ 39.2, 109.9, 111.0, 115.1, 115.9, 117.9, 125.1, 125.4, 127.1, 127.4, 128.7, 149.0, 150.0 and 154.1. Analysis calculated for C₁₇H₁₇N₃O: C, 73.10; H, 6.13; N, 15.04. Found: C, 72.88; H, 5.81; N, 15.01.

1-Carbomethoxy-3-phenyl-5-(3,4,5-trimethoxyphenyl)-1H-pyrazole (12). This compound was prepared by the general procedure described from 0.0100 mol of hydrazone; 2.22 g, 60% yield, m.p. = 176–178°C (methanol/water). FT-IR (paraffin oil): 1763 cm⁻¹. ¹H-NMR (CDCl₃): δ 3.826 (6H, s), 3.855 (3H, s), 3.941 (3H, s), 6.620 (2H, s), 6.662 (1H, s), 7.345–7.391 (3H, m), 7.841 (2H, d). ¹³C-NMR (CDCl₃): δ 54.8, 56.2, 60.9, 106.6, 109.4, 126.0, 126.5, 128.7, 129.3, 131.4, 138.7, 148.4, 150.5, 152.7 and 154.4. Analysis calculated for C₂₀H₂₀N₂O₅: C, 65.21; H, 5.47; N, 7.60. Found: C, 65.09; H, 5.34; N, 7.63.

1-Carbomethoxy-3-(2-methoxyphenyl)-5-(3,4,5-trimethoxyphenyl)-1H-pyrazole (13). This compound was prepared by the general procedure described from 0.0100 mol of hydrazone; 1.32 g, 33% yield, m.p. = 121–124°C (methanol/water). FT-IR (paraffin oil): 1763 cm⁻¹. ¹H-NMR (CDCl₃): δ 3.805 (3H, s), 3.820 (6H, s), 3.841 (3H, s), 3.919 (3H, s), 6.630 (2H, s), 6.874 (1H, s), 6.897 (1H, d), 6.988 (1H, dd), 7.317 (1H, dd), 7.931 (1H, d). ¹³C-NMR (CDCl₃): δ 54.6, 55.5, 56.2, 60.9, 106.7, 111.2, 113.3, 120.4, 120.9, 126.4, 129.5, 130.4, 138.5, 147.1, 150.5, 152.0, 152.7 and 157.4. Analysis calculated for C₂₁H₂₂N₂O₆: C, 63.31; H, 5.57; N, 7.03. Found: C, 63.22; H, 5.45; N, 6.97.

1-Carbomethoxy-5-(4-dimethylaminophenyl)-3-phenyl-1H-pyrazole (14). This compound was prepared by the general procedure described from 0.0100 mol of hydrazone; 1.20 g, 37% yield, m.p. = 105–106°C (95% ethanol). FT-IR (paraffin oil): 1756 cm⁻¹. ¹H-NMR (CDCl₃): δ 2.963 (6H, s), 3.935 (3H, s), 6.593 (1H, s), 6.719 (2H, d), 7.294–7.394 (5H, m), 7.838 (2H, d). ¹³C-NMR (CDCl₃): δ 40.3, 54.6, 108.4, 111.3, 126.5, 128.6, 129.1, 130.0, 131.8, 149.5, 150.6, 150.8 and 154.4. Analysis calculated for C₁₉H₁₉N₃O₃: C, 71.01; H, 5.96; N, 13.07. Found: C, 70.90; H, 5.95; N, 13.05.

Spectroscopy

The UV/visible absorption and fluorescence spectra were recorded on a Perkin-Elmer Lambda 6 spectrophotometer and a Perkin-Elmer LS50 fluorometer, respectively. Spectrograde *n*-heptane was purchased from Aldrich Chemical Co., while 200 proof ethanol and reagent-grade acetonitrile were purchased from Baxter Diagnostics Inc., Scientific Products Division. All solvents were used without further purification.

Relative fluorescence quantum yields (Φ_f) were estimated using quinine sulfate in 1 N H₂SO₄ as the reference standard (Φ_f = 0.55) (32). In order to account for differences in absorbance and refractive index between the sample and the reference, the following equation (33) was used:

$$\Phi_f = \Phi_f^{\text{ref}} (A^{\text{ref}}/A) (n_D/n_D^{\text{ref}})^2 (a/a^{\text{ref}})$$

where A is the absorbance at the excitation wavelength, a is the area under the emission curve, Φ_f is the fluorescence quantum yield and

n_D is the refractive index of the solvent. The variables attributed to the reference are designated by a superscript ref.

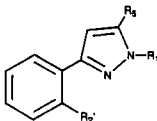
The proton transfer emission is measured in *n*-heptane using a 1 mm pathlength between the cuvette and the monochromator (0.25 m). The excitation wavelength is a 266 nm pulse from the fourth harmonic of a Q-switched Nd:YAG laser. Our entrance and exit slits were 500 μ m and a band-pass filter (Schott OG 515) blocking wavelengths <500 nm was placed between the cuvette and the entrance slit. The emission was detected perpendicular to the excitation pulse by a photomultiplier tube (Oriel 77341) that has a response region from 185 to 870 nm. With these experimental conditions, the spectral resolution is 3–5 nm.

RESULTS AND DISCUSSION

Synthesis

During the investigation, 2'-hydroxyacetophenone carbomethoxyhydrazone was prepared and trilitiated with excess LDA, and the resulting intermediate was treated with a variety of benzoate esters ranging from methyl benzoate to methyl 4-chlorobenzoate to ethyl 4-dimethylaminobenzoate. The resulting *C*-acylated intermediates were quenched with dilute hydrochloric acid and cyclodehydrated to the substituted pyrazoles 1–11. The yields of products ranged from 27 to 94%, which indicates that the electron withdrawal of the *N*-carbomethoxy group in each *C*-acylated intermediate did not significantly hinder cyclodehydration to the substituted heteroaromatic pyrazole product. Due to the electron-donating ability of the 4-dimethylaminophenyl group, the procedure for preparing *N*-carbomethoxypyrazole 10 was modified so as to cause hydrolysis and then decarboxylation of the *N*-carbomethoxy group, and *N*-H pyrazole 11 was isolated in 79% yield instead. This type of hydrolysis/decarboxylation has proven to be more difficult than originally perceived (34), and the initial result merits further study. The condensation/cyclization of the trianion-type intermediate with more challenging esters such as methyl 4-bromobenzoate to 4, or the condensation with other electron-enriched esters, such as ethyl 4-aminobenzoate, to give 5 and 7–10 did not present a problem. Substituted pyrazoles 12–14 were also prepared for comparison purposes in 33–67% yield, because they were related to pyrazoles 8 and 10, and they would be incapable of undergoing ESIPT. Their preparation involved a more routine preparation where a dilithiated carbomethoxyhydrazone, prepared in excess LDA, was condensed/cyclized with either methyl 3,4,5-trimethoxybenzoate (for 12 and 13) or ethyl 4-dimethylaminobenzoate (for 14).

While *N*-phenylpyrazoles (35,36), *N*-H pyrazoles (37) and isoxazole analogs (38) with the *ortho*-hydroxyphenyl in the C-3 position of the heterocyclic ring are known, every compound prepared in this investigation is new, and each was characterized by absorption spectra, including FT-IR, ¹H NMR and ¹³C NMR. The FT-IR spectra displayed dominant and distinct carbomethoxy absorptions ranging between 1727 and 1763 cm^{-1} , and two sharp NH₂ absorptions in 9 were noted at 3476 and 3373 cm^{-1} . The ¹H NMR displayed a carboxy OCH₃ singlet for every compound, ranging between δ 3.90 and 3.97 ppm, and pendant ArOCH₃ in 5–8 were noted as singlets ranging from δ 3.81 to 3.94 ppm; ArCH₃ protons in 2 were noted at δ 2.42 ppm; (CH₃)₂N in 10 was observed at δ 3.01 ppm, at 2.98 ppm in 11 and at 2.96 ppm in 14; NH₂ in 9 was noted at δ 5.48 ppm. Important OH absorptions for the *ortho*-hydroxyphenyl substituent



Compound	R ₁	R ₅	R ₂ '
1	COOCH ₃	phenyl	OH
2	COOCH ₃	4-methylphenyl	OH
3	COOCH ₃	4-chlorophenyl	OH
4	COOCH ₃	4-bromophenyl	OH
5	COOCH ₃	3,5-dimethoxyphenyl	OH
6	COOCH ₃	4-methoxyphenyl	OH
7	COOCH ₃	3,4-dimethoxyphenyl	OH
8	COOCH ₃	3,4,5-trimethoxyphenyl	OH
9	COOCH ₃	4-aminophenyl	OH
10	COOCH ₃	4-dimethylaminophenyl	OH
11	H	4-dimethylaminophenyl	OH
12	COOCH ₃	3,4,5-trimethoxyphenyl	H
13	COOCH ₃	3,4,5-trimethoxyphenyl	OCH ₃
14	COOCH ₃	4-dimethylaminophenyl	H

Figure 1. Structure of 3-(2-hydroxyphenyl)-1H-pyrazoles with various substitutions.

in 1–11 bonded to C-3 on the heterocyclic ring were noted as well-defined (1H) and sharp singlets ranging from δ 10.49 to 10.84 ppm. The focus of the ¹³C for 1–11 is on the following carbons in each molecule: the *ortho*-hydroxyphenyl carbon ranging from δ 153.0 to 156.9 ppm; the C-4 carbon of the pyrazole ring, δ 107.6–110.3 ppm (δ 106.7–108.4 in 13 and 14); the C-3 and C-5 heteroaromatic carbons absorbed in the region δ 146.7–154.1 ppm and higher resolution spectra would be required to distinguish isochronous resonance absorptions in the starting material and compounds 3 and 14 that had one less carbon resonance than expected; the *N*-carbonyl carbon at δ 156.5–160.4 ppm; the methoxy ester carbon at δ 55.0–55.3 ppm; and the *N*-methyl carbon displayed at δ 40.4 ppm in 10, δ 39.2 ppm in 11 and δ 40.3 ppm in 14.

Absorption spectra

As shown in Fig. 1, the compounds 1–11 studied are structurally similar in that they all have an intramolecular hydrogen bond but differ in the degree of the electron-donating ability involved through the R₅ substituent of the pyrazole ring. The two extremes being compound 1 with no electron-donating groups in a resonance position on R₅ compared to compounds 10 and 11 where R₅ is 4-dimethylaminophenyl. The UV/visible absorption spectra for 1–11 were measured in three solvent systems; *n*-heptane (nonpolar), acetonitrile (polar, aprotic) and ethanol (polar, protic) with the absorption maxima and molar absorptivities reported in Table 1. Figure 2 shows the absorption spectra of 1, 9, 10 and 11 in *n*-heptane. The lowest energy absorption maximum for compounds 1, 9, and 11 are all at \sim 303 nm while 10 showed a red-shifted maximum at 314 nm. Associated with this energy difference of 1156 cm^{-1} in the absorption maximum, the molar absorptivity of 10 is 1.5 times larger than that for 1. Both the red shift and the increased molar absorptivity are attributed to a significant degree of charge transfer character that is introduced through the electron-donating ability and resonance effect of the 4-dimethylamino substituent.

The solvent dependency for this series of compounds (1–11) in Table 1 is not what is expected. As the electron-donating ability of the substituent increases, one would expect the charge transfer character to increase and in turn, the absorption maximum to shift to longer wavelengths as the polarity of the solvent increased. Table 1 actually shows that the absorption maxima in acetonitrile and ethanol are blue

Table 1. Spectroscopic data for 3-(2-hydroxyphenyl)-1*H*-pyrazole derivatives at 298 K

Sample (substituents on R ₅)	Solvent	λ_{\max} (abs) (nm)	Log ₁₀ ϵ	λ_{\max} (fluor) (nm)	Stokes shift (cm ⁻¹)	Φ_f
1	Heptane	310	4.02	335	2407	0.00033
	Acetonitrile	302	3.91	365	5715	0.0030
	Ethanol	304	3.97	355	4726	0.00031
2 (4-methyl)	Heptane	306	4.27	361	4979	0.00060
	Acetonitrile	300	4.46	358	5400	0.0040
	Ethanol	302	4.47	356	5022	0.00026
3 (4-chloro)	Heptane	308	4.40	361	4766	0.0020
	Acetonitrile	302	4.15	376	6516	0.0060
	Ethanol	304	4.34	345	3909	0.00098
4 (4-bromo)	Heptane	308	4.07	356	4377	0.00080
	Acetonitrile	300	4.35	376	6737	0.0030
	Ethanol	302	4.51	355	4943	0.00068
5 (3,5-dimethoxy)	Heptane	306	4.55	355	4511	0.00030
	Acetonitrile	300	4.00	396	8080	0.0010
	Ethanol	302	4.27	346	4210	0.0020
6 (4-methoxy)	Heptane	306	4.04	350	4108	0.00034
	Acetonitrile	300	4.12	372	6451	0.0010
	Ethanol	298	4.20	360	5779	0.0020
7 (3,4-dimethoxy)	Heptane	306	4.09	363	5132	0.0019
	Acetonitrile	302	4.12	407	8542	0.0060
	Ethanol	302	4.25	404	8359	0.0070
8 (3,4,5-trimethoxy)	Heptane	306	4.33	370	5653	0.0020
	Acetonitrile	298	4.09	420	9747	0.0060
	Ethanol	300	4.25	416	9294	0.02
9 (4-amino)	Heptane	306	4.06	386	6773	0.0067
	Acetonitrile	308	4.25	440	9740	0.070
	Ethanol	308	4.44	445	9995	0.0095
10 (4-dimethylamino)	Heptane	315	4.21	383	5636	0.0065
	Acetonitrile	312	4.39	620	15 617	<10 ⁻⁵
	Ethanol	312	4.18	453	9976	0.12
11 (4-dimethylamino)	Heptane	306	3.58	357	4669	0.050
	Acetonitrile	306	4.66	373	5870	0.16
	Ethanol	306	4.76	365	5283	0.040

shifted relative to those in *n*-heptane for all compounds except **9** and **11**. The observed blue-shifted absorption maxima are attributed to a change in dipole moment upon ESICT before the solvent can reorient itself to the new electron distribution in the excited state. The difference in stability between the ground and excited states is most pronounced in polar solvents in which the spectral maximum is blue shifted with increasing solvent polarity indicating a destabi-

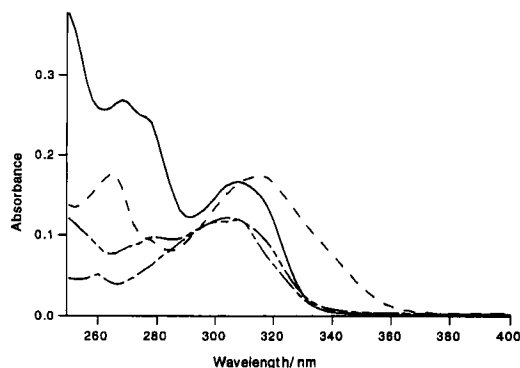


Figure 2. The absorption spectra of compounds **1** and **9–11** in *n*-heptane. The concentrations of the solutions are 10⁻⁵ M. (—) Compound **1**; (---) compound **9**; (-·-·) compound **10**; (·-·-·) compound **11**.

lization of the excited state upon prompt excitation. These results agree with the fluorescence data reported in the next section in that following ESICT one would expect the solvent to realign itself relative to the excited-state dipole moment prior to fluorescence and that the fluorescence maximum would be red shifted with increasing solvent polarity.

Fluorescence spectra

The fluorescence spectra of **1–11** were also taken in *n*-heptane, acetonitrile and ethanol. The fluorescence maxima, Stokes shift (calculated from the lowest energy absorption maximum to the fluorescence maximum) and fluorescence quantum yields are reported in Table 1. In *n*-heptane the spectra are structureless and in general have very low fluorescence quantum yields (10⁻⁴). For simplicity, representative fluorescence spectra are shown in Fig. 3 for compounds **1**, **10** and **11**. The fluorescence maxima listed in Table 1 indicate that there is a trend toward longer wavelengths as the electron-donating ability and number of electron-donating groups on R₅ increases. This is most obvious between the unsubstituted R₅ in **1** with a maximum at 335 nm compared to the 4-dimethylamino-substituted R₅ in **10** with a maximum at 383 nm (see Fig. 1). Another interesting set of compounds to compare are **5**, **6**, **7** and **8** that all have various numbers of methoxy groups on the phenyl ring of R₅. The

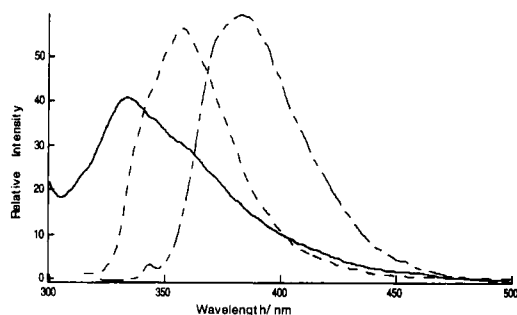


Figure 3. The fluorescence spectra of compounds **1**, **10** and **11** in *n*-heptane. The concentrations of the compounds are 10^{-5} M. (—) Compound **1**; (---) compound **10**; (- -) compound **11**.

trend observed is that the 3,4,5-trimethoxyphenyl-substituted derivative has the longest red shift with its maximum at 370 nm that is followed by 3,4-dimethoxyphenyl at 363 nm, 3,5-dimethoxyphenyl at 355 nm and lastly 4-methoxyphenyl at 350 nm. The fluorescence quantum yields of **5**, **6**, **7** and **8** correlate well with the trend observed for the red-shifted fluorescence maxima by increasing from $\sim 3.0 \times 10^{-4}$ for **5** and **6** to $\sim 2.0 \times 10^{-3}$ for **7** and **8**.

The red shift is reasonably attributed to the increasing charge transfer character that results in a partial double bond between the pendant group R_5 and the rest of the pyrazole molecule. The structure that results from the charge transfer is more rigid and nonradiative losses due to torsional motion of R_5 are reduced, which consequently leads to higher fluorescence quantum yields. The series of methoxyphenyl derivatives offers the opportunity to investigate the effect of position and the number of substituents on electron donation to the overall π system. A methoxy group in the 4-position is an ideal location for the substituent to donate electrons to the π system *via* resonance. Methoxy groups in the 3 or 5 position on the phenyl ring can increase the electron density of the overall π system through the π electrons of the methoxy oxygen, but this effect is not as great as the resonance-donating effect. Considering both the magnitude of the red shift and the increase in fluorescence quantum yield, it appears that the net effect on the overall π system is the same whether there are two methoxy groups in the 3 and 5 position or one methoxy group in the 4-resonance position. A more favorable situation for charge transfer is to keep the methoxy group in a resonance position and add another methoxy group that can contribute weakly through the π electrons of the oxygen. As one would expect, the greatest degree of charge transfer is seen for 3,4,5-trimethoxyphenyl (**8**), with a red shift relative to the 4-methoxyphenyl derivative (**6**) corresponding to an energy of 1545 cm^{-1} .

Another interesting comparison is between compound **10** and **11** that both possess 4-dimethylaminophenyl as R_5 but **11** has been decarboxylated. Compound **10** shows a red-shifted emission at 383 nm implying that there is a significant amount of charge transfer occurring. Compound **11** has an emission maximum at 357 nm that is red shifted compared to the unsubstituted **1** but not to the same extent as **10**. A possible explanation is that the carbomethoxy group acts as an electron-withdrawing group and facilitates charge transfer by pulling electrons through the conjugated system.

The methylated derivative of **8**, 1-carbomethoxy-3-(2-

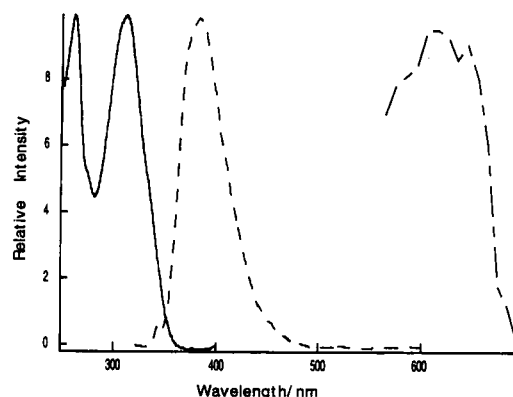


Figure 4. Absorption and fluorescence spectra of compound **10** in *n*-heptane. The concentrations for the absorption and charge transfer spectra are 10^{-5} M while the concentration for the proton transfer spectrum is 10^{-3} M. (—) Absorption; (---) charge transfer; (- - -) proton transfer.

methoxyphenyl)-5-(3,4,5-trimethoxyphenyl)-1*H*-pyrazole **13**, and the derivatives of **8** and **10** without the phenolic hydrogen, 1-carbomethoxy-3-phenyl-5-(3,4,5-trimethoxyphenyl)-1*H*-pyrazole **12** and 1-carbomethoxy-5-(4-dimethylaminophenyl)-3-phenyl-1*H*-pyrazole **14**, were synthesized to elucidate whether IMHB is indeed a significant nonradiative pathway and whether the normal or tautomer excited singlet states are involved in the relaxation dynamics. The emission maxima for compounds **12–14** in *n*-heptane are similar to their IMHB counterparts, but the fluorescence quantum yields are substantially higher. For compounds **12–14** the Φ_f were measured to be 0.30, 0.28 and 0.88 compared to compounds **8** and **10** that possess IMHB and have Φ_f of 2.0×10^{-3} and 6.5×10^{-3} . This nearly 100-fold increase in the normal fluorescence quantum yield concludes IMHB to be a major nonradiative pathway involved in the $S_1 \rightarrow S_0$ relaxation.

In polar solvents, the results in Table 1 show that the fluorescence maxima are further red shifted and the fluorescence quantum yields increase substantially. For example, comparing the data obtained in acetonitrile for **1** and **10**, the fluorescence maxima are 365 and 460 nm and the fluorescence quantum yields are 3.1×10^{-3} and 0.12, respectively. The red-shifted fluorescence is to be expected because the excited state resulting from charge transfer would be further stabilized in a polar solvent. The higher fluorescence quantum yields could be attributed to a solvent cage that surrounds the charge transfer state in a polar environment that further restricts the torsional motion between the pendant group R_5 and the rest of the pyrazole molecule.

Figure 4 presents spectra for **10** in *n*-heptane including the absorption (315 nm), charge transfer fluorescence (383 nm) and an additional fluorescence maximum with a phenomenal Stokes shift (620 nm) corresponding to an energy of 15617 cm^{-1} . This weak, long-wavelength fluorescence was measured using a 1 mm pathlength between the cuvette and the monochromator in combination with a short-wavelength cut-off filter to block emission and/or scattering wavelengths below 500 nm. Catalan *et al.* also observed a long-wavelength fluorescence for several 3-(2'-hydroxyphenyl)pyrazoles with a maximum at ~ 625 nm, which they

attribute to ESIPT from the phenolic OH to the nitrogen in the pyrazole ring (5,6). Based on the similarities between the compounds and the observed spectra, the fluorescence maximum at 620 nm is unambiguously assigned to the tautomer resulting from ESIPT. To substantiate this assignment further, the long-wavelength band at 620 nm was not observed for compound **14** that does not possess a phenolic hydrogen and therefore ESIPT is prohibited.

In theory, all of the compounds **1–11** are structurally capable of undergoing ESIPT. The O–H ¹H NMR shifts for these compounds appearing between δ 10.49–10.84 ppm supports a structure with the phenolic proton bonded to the oxygen but also interacting with the nitrogen in the pyrazole ring (O–H...N). Despite the presence of an IMHB for all the compounds **1–11**, **10** was the only compound that had a detectable amount of fluorescence at 620 nm. Compound **10** does have the strongest O–H...N interaction of compounds **1–10** based on the idea that the farther the shift downfield in the NMR spectrum the stronger the IMHB (39,40). In addition, the efficient electron-donating ability of the dimethylaminophenyl substituent increases the charge transfer character and in turn minimizes nonradiative losses through torsional motion. Note that ESIPT fluorescence was not observed for **11** that also has a dimethylamino substituent in a resonance position; however, it has been decarboxylated. As previously discussed, the carbomethoxy group may pull electrons through the conjugated system and enhance charge transfer. It is also possible that the detection of tautomer fluorescence for **10** and not **11** is due to an intramolecular hydrogen bond existing for the tautomer form of compound **10** between ⁺N–H...O=C making the proton transfer moiety more rigid. So even though ESIPT is a possible excited-state pathway for compounds **1–9** and **11**, there is not enough tautomer fluorescence to detect under our current experimental conditions.

In acetonitrile, the 620 nm proton transfer emission cannot be resolved for compound **10**. In this case, even though there is a significant amount of charge transfer ($\Phi_f = 0.12$), it now interferes with detecting the weak proton transfer fluorescence. At concentrations of 10^{-3} M needed to detect ESIPT, the short-wavelength fluorescence with a maximum at 460 nm will tail down past 500 nm causing interference with the ESIPT fluorescence in a steady-state measurement. Alternatively, it is also possible that in polar solvents the solvated excited, charge transfer state may even cause a reversal in the relative energies of the normal and tautomer states. The outcome would be an energetically unfavorable ESIPT state (12,15). In the case of a polar, protic solvent like ethanol, the absence of ESIPT for **10** is likely due to intermolecular hydrogen bonds formed between the phenolic OH and ethanol (12,15). This solvent perturbation inhibits ESIPT even though charge transfer is favorable.

CONCLUSIONS

The strong base synthetic procedure presents a reproducible method for the preparation of 5-substituted 3-(2-hydroxyphenyl)-1H-pyrazoles in gram quantities. The fluorescence data reported in Table 1 show that it is feasible to fine tune the photophysical properties by electron donor/acceptor strength of substituents, as well as solvent polarity. Even

though there is a significant nonradiative relaxation involving IMHB, the intensity of the fluorescence can be manipulated by increasing the charge transfer character of a molecule and in turn, minimizing the radiationless pathways due to torsional motion. The degree of charge transfer for 2-(1-carbomethoxy-5-[4-dimethylaminophenyl]-1H-pyrazol-3-yl)phenol actually induces ESIPT resulting in a phenomenally large Stokes-shifted fluorescence at 620 nm in *n*-heptane. While the steady-state data presented provide an initial characterization of this new series of pyrazoles, further experiments are necessary to understand fully the excited-state dynamics of this new group of ESIPT/ESICT compounds. From a more general perspective, the results show that substituents can alter the excited-state dynamics making certain pathways more favorable.

Acknowledgements—We thank the following sponsors: the National Science Foundation's Research at Undergraduate Institutions through grant 9708014 and the Donors of the Petroleum Research Fund, Administered by the American Chemical Society. The acquisition of the new 300 MHz NMR spectrometer was made possible through the National Science Foundation's Division of Undergraduate Education through grant DUE 9750721.

REFERENCES

1. Kasha, M. (1986) Proton-transfer spectroscopy. Perturbation of the tautomerization potential. *J. Chem. Soc. Faraday Trans. II* **82**, 2379–2392.
2. Barbara, P. F., P. K. Walsh and L. E. Brus (1989) Picosecond kinetic and vibrationally resolved spectroscopic studies of intramolecular excited-state hydrogen atom transfer. *J. Phys. Chem.* **93**, 29–34.
3. Barbara, P. F. and H. D. Trommsdorff (eds.) (1989) Special issue (Spectroscopy and dynamics of elementary proton transfer in polyatomic systems). *Chem. Phys.* **136**, 153–360.
4. Kasha, M., J. Heldt and D. Gormin (1995) Triplet state potentials in the competitive excitation mechanisms of intramolecular proton transfer. *J. Phys. Chem.* **99**, 7281–7284.
5. Catalan, J., F. Fabero, R. M. Claramunt, M. D. Santa Maria, M. de la Concepcion Foces-Foces, F. H. Cano, M. Martinez-Ripoll, J. Elguero and R. Sastre (1992) New ultraviolet stabilizers: 3- and 5-(2'-hydroxyphenyl)pyrazoles. *J. Am. Chem. Soc.* **114**, 5039–5048.
6. Catalan, J., J. Palomar and J. L. G. de Paz (1997) Intramolecular proton or hydrogen-atom transfer in the ground and excited states of 2-hydroxybenzoyl compounds. *J. Phys. Chem. A* **101**, 7914–7921.
7. Simon, J. D. (1988) Time-resolved studies of solvation in polar media. *Acc. Chem. Res.* **21**, 128–134.
8. Barbara, P. F. and W. Jarzeba (1990) Ultrafast photochemical intramolecular charge transfer and excited state solvation. *Adv. Photochem.* **15**, 1–68.
9. Maroncelli, M., J. MacInnis and G. R. Fleming (1989) Polar solvent dynamics and electron-transfer reactions. *Science* **243**, 1674–1681.
10. Lippert, E., W. Rettig, V. Bonacic-Koutecky, F. Heisel and J. A. Mieke (1987) Photophysics of internal twisting. *Adv. Chem. Phys.* **68**, 1–173.
11. Gray, H. B. and J. R. Winkler (1996) Electron transfer in proteins. *Annu. Rev. Biochem.* **65**, 537–561.
12. Chou, P. T., M. L. Martinez and J. H. Clements (1993) The observation of solvent-dependent proton-transfer/charge-transfer lasers from 4'-diethylamino-3-hydroxyflavone. *Chem. Phys. Lett.* **104**, 395–399.
13. Chou, P. T. and M. L. Martinez (1993) Reinvestigation of the photophysics of 2-(2'-hydroxy-4'-diethylaminophenyl)benzothiazole. *Photochem. Photobiol.* **57**, 593–596.
14. Cornelissen-Gude, C. and W. Rettig (1998) Dual fluorescence and multiple charge transfer nature in derivatives of *N*-pyrrolobenzonitrile. *J. Phys. Chem. A* **102**, 7754–7760.

15. Chou, P. T., M. L. Martinez and J. H. Clements (1993) Reversal of excitation behavior of proton-transfer vs. charge-transfer by dielectric perturbation of electronic manifolds. *J. Phys. Chem.* **97**, 2618–2622.
16. Swinney, T. C. and D. F. Kelley (1993) Proton transfer dynamics in substituted 3-hydroxyflavones: solvent polarization effects. *J. Chem. Phys.* **99**, 211–221.
17. Ormson, S. M., R. G. Brown, F. Vollmer and W. Rettig (1994) Switching between charge- and proton-transfer emission in the excited state of a substituted 3-hydroxyflavone. *J. Photochem. Photobiol. A Chem.* **81**, 65–72.
18. Chou, P. T., D. McMorrow, T. J. Aartsma and M. Kasha (1984) The proton-transfer laser. Gain spectrum and amplification of spontaneous emission of 3-hydroxyflavone. *J. Phys. Chem.* **88**, 4596–4599.
19. Chou, P. T. and T. J. Aartsma (1986) The proton-transfer laser. Dual wavelength lasing action in binary dye mixtures involving 3-hydroxyflavone. *J. Phys. Chem.* **90**, 721–723.
20. Catalan, J., E. Mena, F. Fabero and F. Amat-Guerri (1992) The role of the torsion of the phenyl moiety in the mechanism of stimulated ultraviolet light generation in 2-phenylbenzazoles. *J. Chem. Phys.* **96**, 2005–2016.
21. Acuna, A. U., A. Costela and J. M. Munoz (1986) A proton-transfer laser. *J. Phys. Chem.* **90**, 2807–2808.
22. Chou, P. T., S. L. Studer and M. L. Martinez (1991) Practical and convenient 355 nm and 337 nm sharp-cut filters for multi-channel Raman spectroscopy. *Appl. Spectrosc.* **45**, 513–515.
23. Ernsting, N. P. and B. Nikolaus (1986) Dye laser pulse shortening by transient absorption following excited-state intramolecular proton transfer. *Appl. Phys. B* **39**, 155–164.
24. Renschler, C. L. and L. A. Harrah (1985) Reduction of reabsorption effects in scintillators by using solutes with large Stokes shifts. Nuclear Inst. Methods A 235; U.S. Patent 636655 ChemiAbstr. 103, 185647.
25. Sytnik, A. and M. Kasha (1994) Excited-state intramolecular proton transfer as a fluorescence probe for protein bind-site static polarity. *Proc. Natl. Acad. Sci. USA* **91**, 8627–8630.
26. Haroutounian, S. A. and J. A. Katzenellenbogen (1988) Hydroxystilbazoles and hydroxyazaphenanthrenes: photocyclization and fluorescence studies. *Photochem. Photobiol.* **47**, 503–516.
27. Anstead, G. M., K. E. Carlson, P. R. Kym, K. J. Hwang and J. A. Katzenellenbogen (1993) The effect of acceptor group variation on the solvatochromism of donor-acceptor fluorophores. *Photochem. Photobiol.* **58**, 785–794.
28. Katzenellenbogen, J. A. (1995) The development of molecular probes for fluorescence assay, tumor imaging, and structural studies of steroid receptors. *Med. Chem. Res.* **5**, 606–617.
29. Haroutounian, S. A. and J. A. Katzenellenbogen (1995) 4'-Hydroxystyryldiazines—synthesis and fluorescence properties. *Tetrahedron* **51**, 1585–1598.
30. Diwu, Z., Y. Lu, C. Zhan, D. H. Klaubert and R. P. Haugland (1997) Fluorescent molecular probes II. The synthesis, spectral properties and use of fluorescent solvatochromic Dapoxyl dyes. *Photochem. Photobiol.* **66**, 424–431.
31. French, K. L., A. J. Angel, A. R. Williams, D. R. Hurst and C. F. Beam (1998) A new preparation of substituted 4H-1-benzothioopyran-4-ones from C(α), N-benzoylhydrazones or C(α) N-carboalkoxyhydrazones and methyl thiosalicylate. *J. Heterocycl. Chem.* **35**, 45–48.
32. Demas, J. N. and G. A. Crosby (1971) The measurement of photoluminescence quantum yields. A review. *J. Phys. Chem.* **75**, 991–1024.
33. Hanson, K. M., L. Bulang and J. D. Simon (1997) A spectroscopic study of the epidermal ultraviolet chromophore transurocanic acid. *J. Am. Chem. Soc.* **119**, 2715–2721.
34. Church, A. C., M. U. Koller, M. A. Hines and C. F. Beam (1996) The preparation of 1H-pyrazole-1-carboxylic acid, 1,1-dimethylethyl esters from dilithiated C(α),N-hydrazones of hydrazinecarboxylic acid, 1,1-dimethylethyl ester. *Synth. Commun.* **26**, 3659–3669.
35. Ahamad, R., M. Zai-ul-Haq, N. Khan and N. Kausar (1996) Regioselective cyclocondensation reactions leading to phenolic pyrazoles. *Arabian J. Sci. Eng.* **21**, 393–401.
36. Sharma, T. C., S. R. Pawar and N. J. Reddy (1983) Synthesis of some isomeric pyrazoles. *Acta Chim. Hung.* **112**, 159–162.
37. Colotta, V., D. Catarzi, F. Varno, F. Fabrizio, G. Filacchiani, L. Checchi, A. Galli and C. Costagali (1996) Benzodiazepine binding activity of some tricyclic heteroaromatic systems to define the hydrogen bonding strength of proton donors of the receptors site. *Farmaco* **51**, 223–229.
38. Murthy, A. K., K. S. R. K. M. Rao and N. V. S. Rao (1968) Isoxazolyphenols and their absorption spectra. *Aust. J. Chem.* **21**, 2315–2317.
39. Martinez, M. L., W. C. Cooper and P. T. Chou (1992) A novel excited-state intramolecular proton transfer molecule, 10-hydroxybenzo[h]quinoline. *Chem. Phys. Lett.* **193**, 151–154.
40. Kumar, G. A. and M. A. McAllister (1998) Theoretical investigation of the relationship between proton NMR chemical shift and hydrogen bond strength. *J. Org. Chem.* **63**, 6968–6972.